

# Investigation of the Interaction Between *N*-benzyl Piperidones and Bovine Serum Albumin by Spectroscopic Approaches

Xianyong Yu · Qing Yao · Wei Li · Xuecheng Liao · Ying Yang · Heting Liu · Xiaofang Li · Pinggui Yi

Received: 30 October 2011 / Accepted: 12 December 2011 / Published online: 16 October 2012  
© Springer Science+Business Media New York 2012

**Abstract** Fluorescence and ultraviolet spectroscopies were applied to investigate the interaction between five *N*-benzyl piperidones (NBP) and bovine serum albumin (BSA) under imitated physiological conditions. The experimental results show that these NBPs have a static fluorescence quenching effect on the endogenous fluorescence of BSA at the temperatures 302 and 310 K. According to the fluorescence quenching theory, the Stern–Volmer quenching constant ( $K_{SV}$ ), the binding constant ( $K_a$ ), and the number of binding sites ( $n$ ) were obtained. Also, the effect of substituents on the binding capacity between NBP and BSA is in the order:  $C_6H_5 < 4-CH_3OC_6H_4 < 4-CH_3C_6H_4 < 2,4-Cl_2C_6H_3 < 4-ClC_6H_4$ . The corresponding thermodynamic parameters ( $\Delta G$ ,  $\Delta H$ , and  $\Delta S$ ) were obtained at two different temperatures and indicate that hydrogen bonding and van der Waals forces play main roles in stabilizing the BSA–NBP complex. The binding distance between the tryptophan residue in BSA and NBP was found to be much  $< 7$  nm based on the Förster theory of non-radiation energy transfer. The effect of NBP on the conformation of BSA was analyzed as well by synchronous fluorescence spectroscopy.

**Keywords** Bovine serum albumin · *N*-benzyl piperidones · Fluorescence spectroscopy · Ultraviolet spectroscopy

---

X. Yu · Q. Yao · X. Liao · Y. Yang · H. Liu · X. Li (✉) · P. Yi (✉)  
Key Laboratory of Theoretical Chemistry and Molecular Simulation of the Ministry of Education,  
Hunan Province College Key Laboratory of QSAR/QSPR, School of Chemistry and Chemical  
Engineering, Hunan University of Science and Technology, Xiangtan 411201, China  
e-mail: fine\_chem@163.com

P. Yi  
e-mail: pgyi@hnust.cn

W. Li  
The 78668 of the Chinese People's Liberation Army, Chengdu 610203, China

## 1 Introduction

Serum albumin (SA) is the most common and important carrier protein in blood plasma, which can extensively bind with many exogenous and endogenous substances. Drug molecules will reach the SA receptor site and have pharmacological effects when being stored and transported via blood plasma inside the human body. Therefore, it is significant to have research into the binding capacity of proteins under different conditions. Because BSA and HSA have a homology of 76 % and have similar 3D structures, BSA is an appropriate protein model to study the interaction between HSA and drugs [1–5]. Investigations of the interaction of SA with drug molecules can lead us to understand the absorption and distribution of the drug [6, 7]. The profound significance of the interaction between drugs and protein in clinical therapy on pharmacodynamics and pharmacokinetics makes this an extraordinarily active field of research [8].

*N*-benzyl piperidones (NBP) are types of pharmaceutical intermediates, which have been widely used in the synthesis of analgesic, anti-inflammatory, anti-histamine, anti-arrhythmia, anti-psychosis, mental disease, and anti-tumor medicines. Its general structure is shown in Scheme 1 [9]. Investigating the interaction of NBP and BSA can provide information on understanding the mechanism of action of NBP on the human body.

Fluorescence spectroscopy is a suitable and helpful way to determine the interaction between small molecules and biomolecules [10]. Through analysis of the fluorescence parameters, some information concerning the structural changes in a biomacromolecule can be gotten. In this paper, UV–Vis and fluorescence techniques were applied to investigate the interaction between bovine SA and five NBP compounds.

## 2 Experimental Details

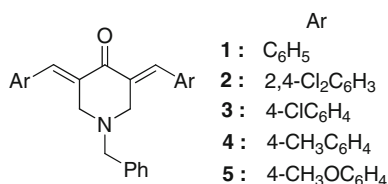
### 2.1 Materials

BSA ( $\geq 99\%$ ) was obtained from Jitian Bioengineering Co. (Shanghai, China) and was dissolved in an aqueous Tris–HCl ( $0.10\text{ mol}\cdot\text{L}^{-1}$ ,  $\text{pH} = 7.37$ ) buffer to form a BSA solution with the concentration  $1.00 \times 10^{-5}\text{ mol}\cdot\text{L}^{-1}$ . The Tris–HCl buffer ( $0.10\text{ mol}\cdot\text{L}^{-1}$ ,  $\text{pH} = 7.37$ ) containing  $0.10\text{ mol}\cdot\text{L}^{-1}$  NaCl was selected to keep the pH value constant and to maintain the ionic strength of the solutions. The NBP solution ( $1.50 \times 10^{-3}\text{ mol}\cdot\text{L}^{-1}$ ) was prepared in DMF. All other reagents were of analytical grade and all of the water used in the experiments was double distilled water.

### 2.2 Apparatus

Fluorescence spectra were recorded on a Shimadzu RF-5301 fluorescence spectrophotometer (Tokyo, Japan) with a SB-11 water bath (Eyela) and 1.0 cm quartz cells. The

**Scheme 1** The structure of NBP



excitation and emission slits were 5 and 10 nm, respectively. The synchronous fluorescence spectra were obtained by setting the excitation and emission wavelength interval ( $\Delta\lambda$ ) at 15 and 60 nm, respectively. The absorption spectra were obtained from a Shimadzu UV-2501 spectrophotometer (Tokyo, Japan). The pH measurement was made with a Leici PHS-2 digital pH-meter (Shanghai, China) with a combined glass–calomel electrode.

### 2.3 Procedures

A 2.5 mL solution, containing the appropriate concentration of BSA ( $1.00 \times 10^{-5} \text{ mol}\cdot\text{L}^{-1}$ ), was titrated by successive additions of NBP solution with concentrations varying from 0 to  $5.40 \times 10^{-5} \text{ mol}\cdot\text{L}^{-1}$ . Titrations were done manually by using a microinjector. Fluorescence spectra were measured in the 280–600 nm range at the excitation wavelength 280 nm at two temperatures (302 and 310 K, with  $\pm 0.1$  K control). The synchronous fluorescence spectra were obtained by scanning the solutions while fixing  $\Delta\lambda$  at 15 and 60 nm.

The UV–Vis absorption spectra of a  $1.00 \times 10^{-5} \text{ mol}\cdot\text{L}^{-1}$  NBP solution were measured in the 200–600 nm range at 302 K.

## 3 Results and Discussion

### 3.1 Fluorescence Quenching Studies of BSA

The condition that drug molecules have biological activity requires that the drug and target molecules interact [11]. In order to investigate the interaction between NBP and BSA, we carried out additions of NBP to a fixed concentration of BSA. The relative decrease of the fluorescence intensity with increase in the NBP concentration at 302 K is plotted in Fig. 1. It can be seen from this figure that the fluorescence intensity of BSA decreases regularly with the addition of NBP and there is an obvious emission wavelength shift. This shows that NBP can interact with BSA and at the same time quench its intrinsic fluorescence [12].

### 3.2 The Mechanism of Quenching of BSA Fluorescence by NBP

Fluorescence quenching can occur via various mechanisms, usually classified as static quenching and dynamic quenching. Static quenching occurs when a non-fluorescent complex of the ground state fluorophore is formed, while dynamic quenching occurs when the fluorophore and the quencher collide with each other during the lifetime of the excited state [13]. For the purpose of examining the quenching mechanism, we first suppose that the fluorescence quenching mechanism is dynamic quenching and that the mechanism can be analyzed by the Stern–Volmer equation as follows [14]:

$$\frac{F_0}{F} = 1 + K_{SV}[Q] = 1 + K_q\tau_0[Q] \quad (1)$$

where  $F_0$  and  $F$  are the relative fluorescence intensities of BSA in the absence and presence of quencher, respectively;  $[Q]$  is the quencher concentration;  $K_q$ ,  $K_{SV}$  and  $\tau_0$  are the bimolecular quenching rate constant, the dynamic quenching constant, and the average lifetime of the molecule without quencher, respectively. According to the Stern–Volmer quenching equation, the Stern–Volmer plots of the quenching of BSA fluorescence by NBP at the two temperatures are shown in Fig. 2.

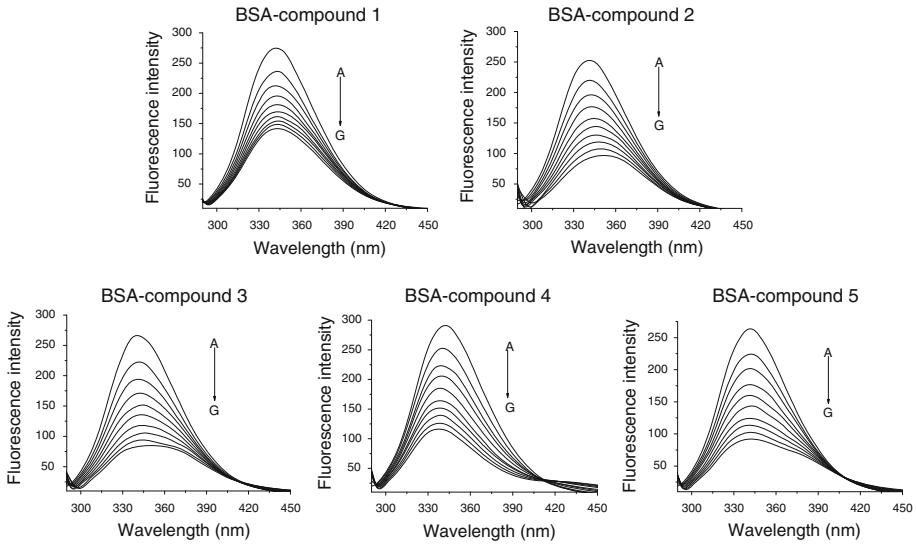


**Fig. 1** Effect of five different NBP compounds on the quenching of BSA fluorescence where  $\lambda_{\text{ex}} = 280 \text{ nm}$  and  $c_{\text{BSA}} = 1.0 \times 10^{-5} \text{ mol}\cdot\text{L}^{-1}$  and  $T = 302 \text{ K}$ ;  $c_{\text{NBP}}$  (a–j) 0.0, 0.6, 1.2, 1.8, 2.4, 3.0, 3.6, 4.2, 4.8, and  $5.4 (\times 10^{-5} \text{ mol}\cdot\text{L}^{-1})$

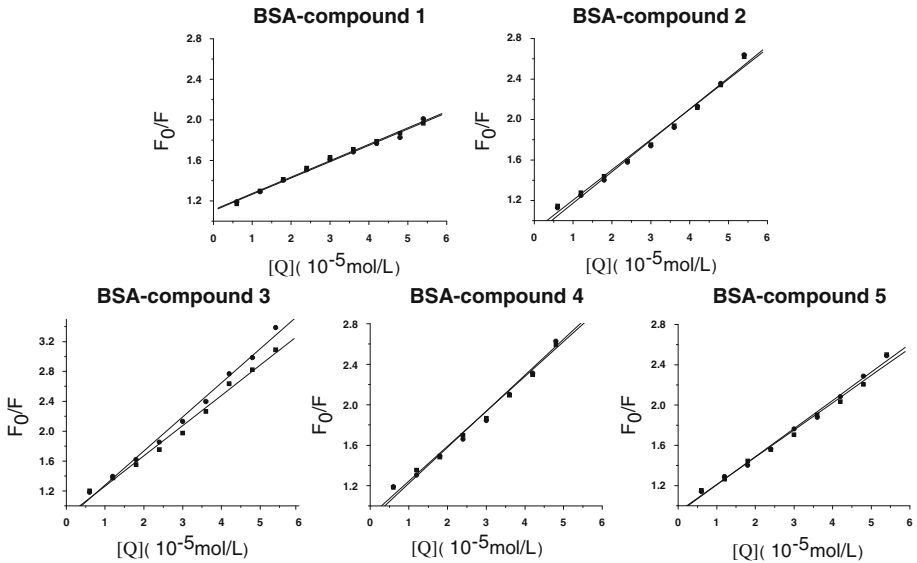


**Fig. 2** Stern–Volmer plots of BSA ( $1.00 \times 10^{-5} \text{ mol}\cdot\text{L}^{-1}$ ) quenched by five NBP compounds at two temperatures (filled square 302 K and filled circle 310 K)

Within a certain concentration range, the curve of  $F_0/F$  versus  $[Q]$  (Stern–Volmer curve) will be linear if the quenching type is single static or dynamic quenching [15]. It can be seen from Fig. 2 that the Stern–Volmer curves are linear. Dynamic and static quenching can be distinguished by the value of the quenching constant  $K_{\text{SV}}$ . According to the

literature [16–18], for dynamic quenching the maximum scatter collision quenching constant of various quenchers with a biopolymer is  $2.0 \times 10^{10} \text{ L}\cdot\text{mol}^{-1}\cdot\text{s}^{-1}$ . That is, if the value of  $K_q$  is much  $>2.0 \times 10^{10} \text{ L}\cdot\text{mol}^{-1}\cdot\text{s}^{-1}$ , it can be concluded that the quenching is not initiated by dynamic quenching, but probably by static quenching, resulting from the formation of a drug–BSA complex. The values of  $K_{SV}$  and  $K_q$  are listed in Table 1. These values show that  $K_{SV}$  decreases with increasing temperature at low concentrations of NBP [19] and the value of  $K_q$  is much larger than  $2.0 \times 10^{10} \text{ L}\cdot\text{mol}^{-1}\cdot\text{s}^{-1}$ . All of the foregoing statement indicates that a static quenching mechanism is operative.

### 3.3 Binding Parameters and Binding Sites

For static quenching, the relationship between fluorescence quenching intensity and the concentration of quenchers can be described by a modified form of the Stern–Volmer equation [20]:

$$\log_{10}\left(\frac{F_0 - F}{F}\right) = \log_{10}K_A + n\log_{10}[Q] \quad (2)$$

where  $K_A$  is the binding constant and  $n$  is the number of binding sites per BSA molecule. Figure 3 shows the double-logarithm curves ( $\log_{10} [(F_0 - F)/F]$  versus  $\log_{10} [\text{NBP}]$ ) that can be used to determine the values of  $K_A$  and  $n$ . Table 2 lists the resulting calculated values of  $K_A$  and  $n$ . The values of  $K_A$  fall in the order: compound 1 < compound 5 < compound 4 < compound 2 < compound 3; this order indicates that compound 3 has the strongest binding capacity while compound 1 has the weakest binding capacity with BSA. All of the substituents on the benzene ring (-2,4-Cl<sub>2</sub>, -4-Cl, -4-CH<sub>3</sub>, -4-OCH<sub>3</sub>) enhanced the binding capacity of NBP with BSA.

We speculate that this may be due to the following two reasons: on one hand, larger drug molecules may contain a relatively larger hydrophobic regions, which can better react with part of the hydrophobic surface of a protein; on the other hand, with increasing electronegativity of the substituent, the affinity increases.

In addition, from the values of  $n$  ( $n \approx 1$ ) it can be inferred that there is one independent class of binding sites on BSA for NBP.

**Table 1** The quenching constants of BSA by different NBP compounds at different temperatures

Compound	<i>T</i> (K)	$K_{SV}$ (L·mol <sup>-1</sup> )	$K_q$ (L·mol <sup>-1</sup> ·s <sup>-1</sup> )	<i>R</i>	<i>SD</i> (× 10 <sup>4</sup> L·mol <sup>-1</sup> )
1	302	$1.61 \times 10^4$	$1.61 \times 10^{12}$	0.9961	0.0402
	310	$1.60 \times 10^4$	$1.60 \times 10^{12}$	0.9954	0.0521
2	302	$3.04 \times 10^4$	$3.04 \times 10^{12}$	0.9947	0.0601
	310	$3.00 \times 10^4$	$3.00 \times 10^{12}$	0.9945	0.0553
3	302	$4.53 \times 10^4$	$4.53 \times 10^{12}$	0.9956	0.0681
	310	$3.89 \times 10^4$	$3.89 \times 10^{12}$	0.9962	0.0744
4	302	$3.50 \times 10^4$	$3.50 \times 10^{12}$	0.9943	0.0647
	310	$3.45 \times 10^4$	$3.45 \times 10^{12}$	0.9945	0.0758
5	302	$2.79 \times 10^4$	$2.79 \times 10^{12}$	0.9967	0.0271
	310	$2.70 \times 10^4$	$2.70 \times 10^{12}$	0.9940	0.0250

*R* is the correlation coefficient, *SD* is the standard deviation for  $K_{SV}$

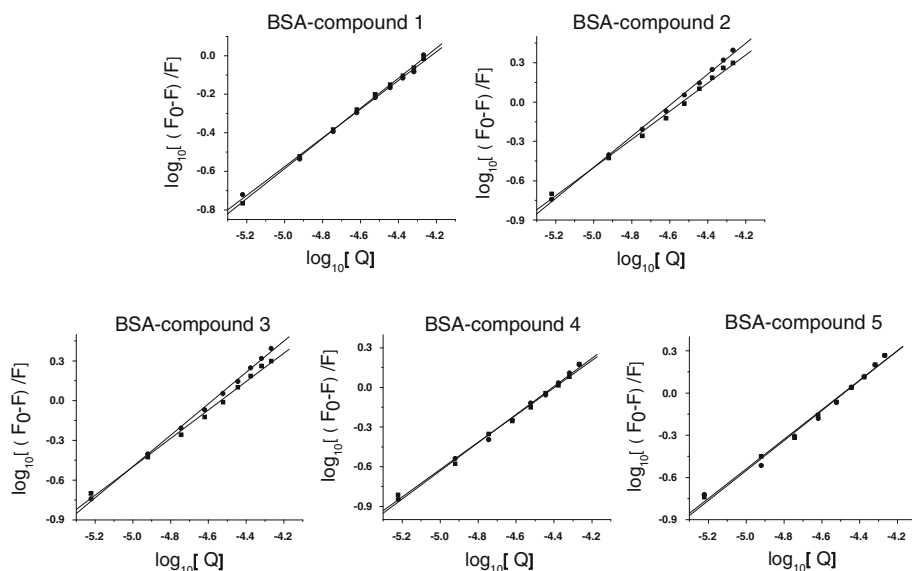


**Fig. 3** Plots of  $\log_{10} [(F_0 - F)/F]$  versus  $\log_{10} [\text{NBP}]$  at two temperatures (filled circle 302 K; filled square 310 K)

**Table 2** The binding constants and the number of binding sites of the five NBP compounds to BSA

System	$T$ (K)	$K_A$ ( $\text{L}^{-1}$ )	$n$	$R$	$SD$ ( $\times 10^4 \text{ L}\cdot\text{mol}^{-1}$ )
BSA-compound 1	302	$2.11 \times 10^3$	0.79	0.9996	0.0126
	310	$1.43 \times 10^3$	0.75	0.9973	0.0075
BSA-compound 2	302	$1.29 \times 10^5$	1.15	0.9981	0.0404
	310	$6.84 \times 10^4$	1.09	0.9981	0.0298
BSA-compound 3	302	$2.63 \times 10^5$	1.18	0.9990	0.0179
	310	$7.43 \times 10^4$	1.07	0.9969	0.0282
BSA-compound 4	302	$5.89 \times 10^4$	1.06	0.9936	0.0075
	310	$5.19 \times 10^4$	1.05	0.9964	0.0182
BSA-compound 5	302	$4.98 \times 10^4$	1.07	0.9981	0.0221
	310	$3.45 \times 10^4$	1.03	0.9965	0.0286

$R$  is the correlation coefficient,  $SD$  is the standard deviation for  $K_A$

### 3.4 Thermodynamic Parameters and the Nature of the Binding Forces

The interaction can be characterized by the thermodynamic parameters  $\Delta G$ ,  $\Delta H$ , and  $\Delta S$ , which can provide evidence to confirm the binding modes. There are actually four types of non-covalent interactions that can play a significant role in drug (and some other organic molecules) binding to a protein: Van der Waals, hydrophobic, hydrogen bonding, and/or electrostatic interactions [21]. The thermodynamic parameters of the system were computed using the van't Hoff equation [22]:

$$\ln K_A = -\frac{\Delta H}{RT} + \frac{\Delta S}{R} \quad (3)$$

Utilizing the binding constants of the system,  $K_A$  values obtained earlier, the values of  $\Delta H$  and  $\Delta S$  can be calculated from the linear relationship between  $\ln K_A$  and the reciprocal absolute temperature, and the Gibbs energy change  $\Delta G$  can be obtained from the following relationship:

$$\Delta G = \Delta H - T\Delta S \quad (4)$$

Numerous studies making use of large quantities of laboratory experiments summarize the binding property's thermodynamic pattern between bio-macromolecules and organic-micromolecule. That is, when  $\Delta S > 0$  there may be hydrogen bonding and/or electrostatic interactions; when  $\Delta S < 0$ , the binding force may be Van der Waals and hydrophobic; when  $\Delta H < 0$  and  $\Delta S < 0$ , the binding force is Van der Waals and hydrophobic;  $\Delta H > 0$  and  $\Delta S > 0$  are typical of hydrogen bonding;  $\Delta H \approx 0$  or  $\Delta S > 0$  and small in value indicates electrostatic interaction; when  $\Delta H < 0$ , electrostatic interaction is the major binding force [22–24]. Regardless of the type of interaction(s), biomolecules and organic molecules in aqueous solution may be solvated.

The values of  $\Delta H$ ,  $\Delta S$  and  $\Delta G$  were calculated and are listed in Table 3. The negative values of  $\Delta G$ ,  $\Delta G < 0$ , indicate that the binding process is spontaneous. That the values of  $\Delta H$  and  $\Delta S$  are also negative indicates that the main binding forces between NBP and BSA are hydrogen bonding and van der Waals.

### 3.5 Energy Transfer

Based on the Förster non-radiative resonance energy transfer theory, if all the following three conditions are met, then energy transfer will happen followed by fluorescence quenching. First, the donor can produce fluorescent; second, the UV absorbance spectrum of the receptor and the fluorescence emission spectrum of the donor significantly overlap; and third, the distance between donor and receptor should be  $< 7$  nm [25]. Based on this theory, the energy transfer efficiency ( $E$ ) is related to the distance of the donor–receptor ( $r$ ) and Förster's critical distance ( $R_0$ ). The efficiency of energy transfer between donor and receptor can be modeled using using equation below:

$$E = 1 - \frac{F}{F_0} = \frac{R_0^6}{R_0^6 + r^6} \quad (5)$$

where  $R_0$  is the critical distance where the energy transfer efficiency is 50 %, and it can be acquired from the donor emission and the receptor absorption spectra using Eq. 6. The dipole orientation factor  $K = 2/3$  if both the donor and acceptor are tumbling rapidly and are free to assume any orientation. In the present case,  $N = 1.336$  and  $\Phi = 0.118$  [26]:

$$R_0^6 = 8.8 \times 10^{-25} K^2 \Phi N^{-4} J \quad (6)$$

where  $K^2$  is the spatial orientation factor,  $N$  the average refractive index of the medium,  $\Phi$  is the quantum yield of the donor in the absence of receptor, and  $J$  the overlap integral of the fluorescence emission spectrum of the donor and the absorption spectra of the receptor, which can be calculated by the following equation:

**Table 3** The thermodynamic parameters of NBP-BSA

System	$T = 302 \text{ K}$			$T = 310 \text{ K}$		
	$\Delta H \text{ (kJ}\cdot\text{mol}^{-1}\text{)}$	$\Delta G \text{ (kJ}\cdot\text{mol}^{-1}\text{)}$	$\Delta S \text{ (J}\cdot\text{mol}^{-1}\cdot\text{K}^{-1}\text{)}$	$\Delta H \text{ (kJ}\cdot\text{mol}^{-1}\text{)}$	$\Delta G \text{ (kJ}\cdot\text{mol}^{-1}\text{)}$	$\Delta S \text{ (J}\cdot\text{mol}^{-1}\cdot\text{K}^{-1}\text{)}$
BSA-compound <b>1</b>	-37.43	-19.22	-61.12	-37.43	-18.73	-61.10
BSA-compound <b>2</b>	-44.75	-29.55	-51.30	-44.75	-28.69	-52.73
BSA-compound <b>3</b>	-122.32	-31.34	-303.98	-122.32	-28.91	-303.90
BSA-compound <b>4</b>	-12.38	-27.58	-50.33	-12.38	-27.98	-50.32
BSA-compound <b>5</b>	-35.37	-27.16	-27.98	-35.37	-26.93	-27.96



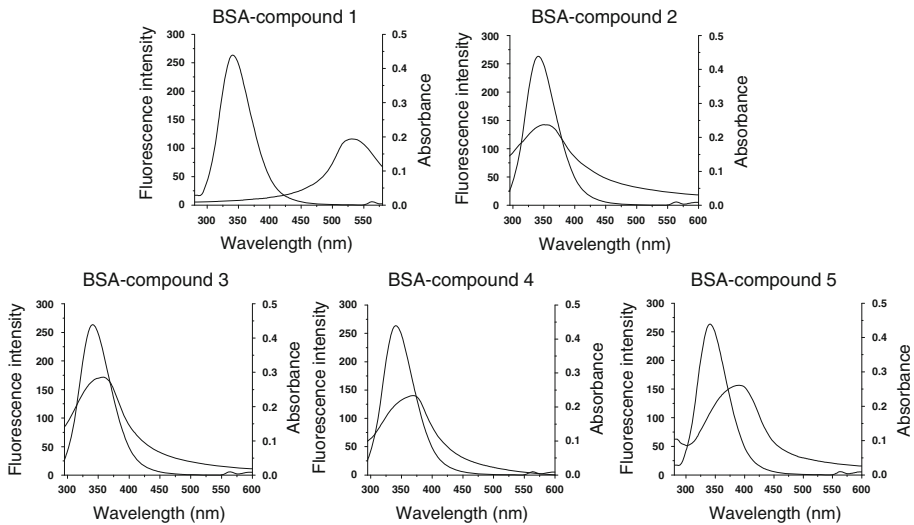


**Fig. 4** Fluorescence spectra for BSA and UV absorbance spectra for the five different NBP compounds:  $c_{BSA} = c_{NBP} = 1.00 \times 10^{-5} \text{ mol}\cdot\text{L}^{-1}$  and  $T = 302 \text{ K}$

**Table 4** The distance parameters between BSA and NBP

System	$J \text{ (cm}^3 \text{ L}\cdot\text{mol}^{-1}\text{)}$	$E$	$R_0 \text{ (nm)}$	$r \text{ (nm)}$
BSA–compound 1	$2.45 \times 10^{-14}$	0.22	2.21	2.73
BSA–compound 2	$3.46 \times 10^{-14}$	0.15	2.35	3.14
BSA–compound 3	$3.69 \times 10^{-14}$	0.22	2.37	2.93
BSA–compound 4	$3.25 \times 10^{-14}$	0.19	2.32	2.95
BSA–compound 5	$2.41 \times 10^{-14}$	0.17	2.20	2.87

$$J = \frac{\sum F(\lambda)\varepsilon(\lambda)\lambda^4\Delta\lambda}{\sum F(\lambda)\Delta\lambda} \tag{7}$$

where  $\lambda$  is the wavelength of the corresponding fluorescence spectrum of BSA and absorption spectrum of NBP.  $F(\lambda)$  is the fluorescence intensity and  $\varepsilon(\lambda)$  is the molar absorptivity of the receptor at wavelength  $\lambda$ .

Results are listed in the table below from calculations based on Fig. 4. We can see in Table 4 that the distance between NBP fluorescent amino acids and BSA is  $<7 \text{ nm}$ . Therefore, non-radiative energy transfer can occur between BSA and all of five small drug molecules.

### 3.6 Conformation Investigation

Synchronous fluorescence spectra can provide effective information about the microenvironment around fluorogens in biomolecules [27]. The excitation wavelengths of Tyr and Trp residues in ordinary spectrum of BSA are 255 and 300 nm, respectively. Concerning the transfer of energy from Tyr to Trp residues, the emission peak positions of the two

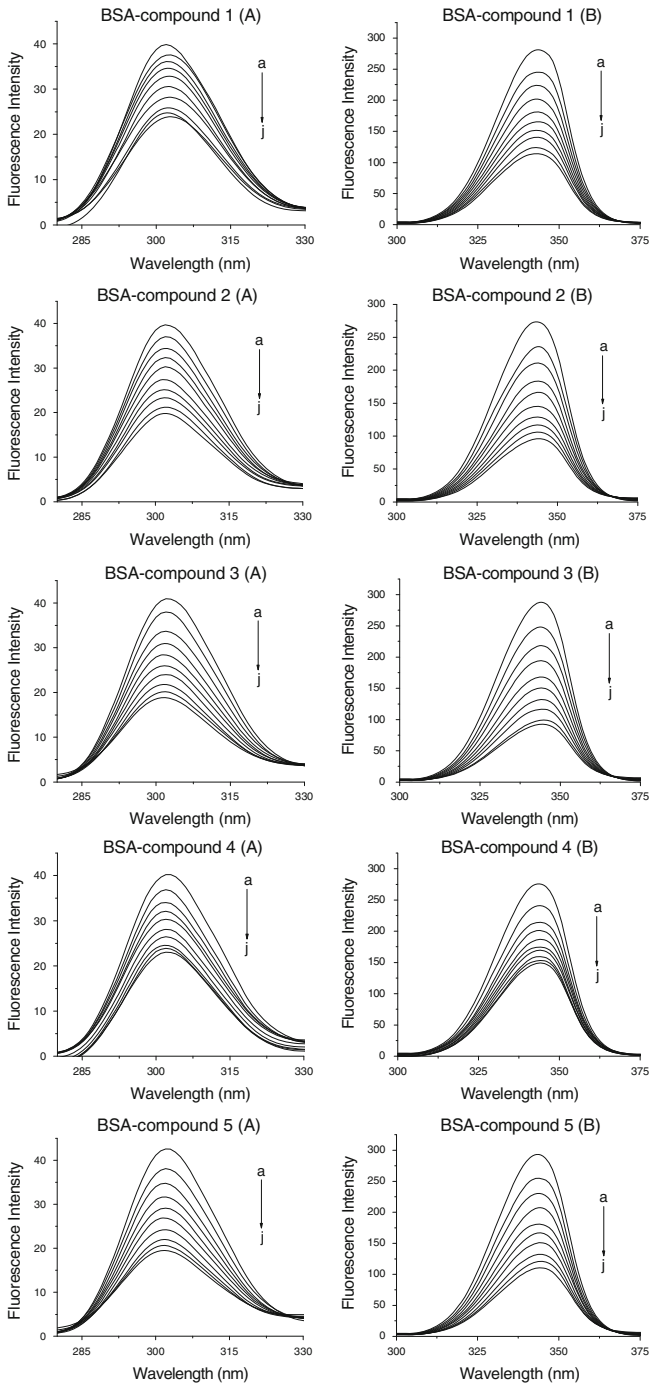


**Fig. 5** Synchronous fluorescence spectroscopy of the effect of NBP on BSA: **a**  $\Delta\lambda = 15$  nm; **b**  $\Delta\lambda = 60$  nm. In all cases  $c_{\text{BSA}} = 1.0 \times 10^{-5}$  mol·L $^{-1}$  and  $T = 302$  K;  $c_{\text{NBP}}$  (**a–j**): 0, 0.6, 1.2, 1.8, 2.4, 3.0, 3.6, 4.2, 4.8, and 5.4 ( $\times 10^{-5}$  mol·L $^{-1}$ )

amino acids are the same, and therefore fluorescence of Tyr and Trp residues can't be distinguished. However, synchronous fluorescence spectroscopy is able to distinguish their peaks. In general, for BSA molecules, when  $\Delta\lambda$  between excitation and emission wavelength is fixed at 15 and 60 nm, respectively, synchronous fluorescence provides characteristic information for the tyrosine residues and tryptophan residues [28].

The synchronous fluorescence quenching curves of BSA solutions titrated with solutions of various concentrations NBP compounds are shown in Fig. 5. The results show that the emission wavelength of Fig. 5 plots A1–A5 have a slight red shift and Fig. 5 plots B1–B5 have a blue shift, revealing that the conformation of BSA has been changed [29].

## 4 Conclusions

In this paper, the interaction of five synthesized NBP compounds with bovine SA (BSA) molecules was investigated by fluorescence and ultraviolet spectroscopy. Examination of the resulting data has revealed that the binding increases with increasing concentration of NBP at low drug–protein ratios. The obtained experimental results suggest that 4 of the substituents on the benzene ring have great influence on the binding constant and the binding force between NBP and BSA, which is predominantly due to the Van der Waals force. In order to evaluate the association constant  $K_A$  and the number of binding sites  $n$ , the double-logarithm curves were constructed. Due to the effect of substituents, the binding capacity falls in this order:  $-C_6H_5 < -4-OCH_3C_6H_4 < -4-CH_3C_6H_4 < -2,4-Cl_2C_6H_3 < -4-ClC_6H_4$ . The values of  $n$  are near 1, so there is only one binding site between NBP and BSA. Furthermore, as their binding distance is  $<7$  nm, non-energy transfer occurs. Synchronous fluorescence spectra show both red and blue shifts, which are evidence of an effect on the conformation of BSA. This study is expected to have certain practical significance to the interactions of the physiologically important protein SA with NBP compounds.

**Acknowledgments** This work was supported by the National Natural Science Foundation of China (20803020, 20971041, 21172066), Scientific Research Fund of Hunan Provincial Education Department (09K081, 12K101), Key Project of Chinese Ministry of Education (210146), Hunan Provincial Natural Science Foundation of China (11JJ2007), Open Project Program of Key Laboratory of Theoretical Chemistry and Molecular Simulation of Ministry of Education (Hunan University of Science and Technology).

## References

1. Yang, J., Jing, Z.H., Jie, J.J., Guo, P.: Fluorescence spectroscopy study on the interaction between gossypol and bovine serum albumin. *J. Mol. Struct.* **920**, 227–230 (2009)
2. Xu, H., Gao, S.L., Lv, J.B., Liu, Q.W., Zuo, Y., Wang, X.: Spectroscopic investigation on the mechanism of interaction of crystal violet with bovine serum albumin. *J. Mol. Struct.* **919**, 334–338 (2009)
3. Hu, Y.J., Yu, H.G., Dong, J., Yang, X., Liu, Y.: Spectroscopic studies on the interaction between 3,4,5-trimethoxybenzoic acid and bovine serum albumin. *Spectrochim. Acta A* **65**, 988–992 (2006)
4. Guo, X.J., Sun, X.D., Xu, S.K.: Spectroscopic investigation of the interaction between riboflavin and bovine serum albumin. *J. Mol. Struct.* **931**, 55–59 (2009)
5. Gelamo, E.L., Tabak, M.: Interaction of bovine (BSA) and human (HSA) serum albumins with ionic surfactants: spectroscopy and modeling. *Spectrochim. Acta A* **56**, 2255–2271 (2000)
6. Ahmad, B., Parveen, S., Khan, R.H.: Effect of albumin conformation on the binding of ciprofloxacin to human serum albumin: a novel approach directly assigning binding site. *Biomacromolecules* **7**, 1350–1356 (2006)
7. Sevilla, P., Rivas, J.M., Garcia-Blanco, F., Garcia-Ramos, J.V., Sanchez-Cortes, S.: Identification of the anti tumoral drug emodin binding sites in bovine serum albumin by spectroscopic methods. *Biochim. Biophys. Acta* **1774**, 1359–1369 (2007)

8. Guo, M., Zou, J.W., Yi, P.G., Shang, Z.C., Hu, G.X., Yu, Q.S.: Binding interaction of gatifloxacin with bovine serum albumin. *Anal. Sci.* **20**, 465–470 (2004)
9. Li, X.F., Yu, X.Y., Yi, P.G.: Synthesis of novel trispiroheterocycles through 1,3-dipolar cycloaddition of azomethine ylides and nitrile oxide. *Chin. J. Chem.* **28**, 434–438 (2010)
10. Soares, S., Mateus, N., Freitas, V.: Interaction of different polyphenols with bovine serum albumin (BSA) and human salivary  $\alpha$ -amylase (HSA) by fluorescence quenching. *J. Agric. Food Chem.* **55**, 6726–6735 (2007)
11. Guo, M., Zou, J.W., Yi, P.G., Shang, Z.C., Hu, G.X., Yu, Q.S.: Binding interaction of gatifloxacin with bovine serum albumin. *Anal. Lett.* **20**, 465–470 (2004)
12. Shaikh, S.M.T., Seetharamappa, J., Kandagal, P.B., Manjunath, D.H., Ashoka, S.: A study of the adsorption of dyes on bovine serum albumin by the method of polarization of fluorescence. *Dyes Pigments* **74**, 665–671 (2007)
13. Moreno, F., Gonzalez-Jimenez, J.: Fluorescence quenching studies on binding fluoreno-9-spiro-oxazolinedione to human serum albumin. *Chem. Biol. Interact.* **121**, 237–252 (1999)
14. Hu, Y.J., Liu, Y., Wang, J.B., Xiao, X.H., Qu, S.S.: Studies on the interaction between 1-hexylcarbamoyl-5-fluorouracil and bovine serum albumin. *J. Pharm. Biomed. Anal.* **36**, 915–919 (2004)
15. Lakowicz, J.R.: Principles of fluorescence spectroscopy, 3rd edn, pp. 278–330. Springer, New York (2006)
16. Xiao, J.B., Suzuki, M., Jiang, X.Y., Chen, X.Q., Yamamoto, K., Xu, M.: Influence of B-ring hydroxylation on interactions of flavonols with bovine serum albumin. *J. Agric. Food Chem.* **56**, 2350–2356 (2008)
17. Xiao, J.B., Shi, J., Cao, H., Wu, S.D., Ren, F.L., Xu, M.: Analysis of binding interaction between puerarin and bovine serum albumin by multi-spectroscopic method. *J. Pharm. Biomed.* **45**, 609–615 (2007)
18. Xiao, J.B., Chen, J.W., Cao, H., Ren, F.L., Yang, C.S., Chen, Y., Xu, M.: Study of the interaction between baicalin and bovine serum albumin by multi-spectroscopic method. *J. Photochem. Photobiol., A* **191**, 222–227 (2007)
19. Zhang, Y.Z., Xiang, X., Mei, P., Dai, J., Zhang, L.L., Liu, Y.: Spectroscopic studies on the interaction of Congo Red with bovine serum albumin. *Spectrochim. Acta A* **72**, 907–914 (2009)
20. Hu, Y.J., Liu, Y., Jiang, W., Zhao, R.M., Qu, S.S.: Fluorometric investigation of the interaction of bovine serum albumin with surfactants and 6-mercaptopurine. *J. Photochem. Photobiol. B* **80**, 235–242 (2005)
21. Klotz, I.M.: Physicochemical aspects of drug–protein interactions: a general perspective. *Ann. N.Y. Acad. Sci.* **226**, 18–35 (1973)
22. Tian, J., Liu, J., He, W., Hu, Z., Yao, X., Chen, X.: Probing the binding of scutellarin to human serum albumin by circular dichroism, fluorescence spectroscopy, FTIR, and molecular modeling method. *Biomacromolecules* **5**, 1956–1961 (2004)
23. Ross, P.D., Subramanian, S.: Thermodynamics of protein association reactions: forces contributing to stability. *Biochemistry* **20**, 3096–3102 (1981)
24. Yue, Y., Zhang, Y., Qin, J., Chen, X.: Study of the interaction between esculetin and human serum albumin by multi-spectroscopic method and molecular modeling. *J. Mol. Struct.* **888**, 25–32 (2008)
25. Stryer, L.: Fluorescence energy transfer as a spectroscopic ruler. *Ann. Rev. Biochem.* **47**, 819–846 (1978)
26. Cui, F.L., Fan, J., Li, J.P., Hu, Z.: Interactions between 1-benzoyl-4-*p*-chlorophenyl thiosemicarbazide and serum albumin: investigation by fluorescence spectroscopy. *Bioorg. Med. Chem.* **12**, 151–157 (2004)
27. Yuan, T., Weljie, A.M., Vogel, H.J.: Spectroscopic characterization of the calmodulin-binding and autoinhibitory domains of calcium/calmodulin-dependent protein kinase I. *Biochemistry* **37**, 3187–3195 (1998)
28. Miller, J.N.: Recent advances in molecular luminescence analysis. *Proc. Anal. Div. Chem. Soc.* **16**, 203–208 (1979)
29. Zhang, Y.Z., Zhou, B., Liu, Y.X., Zhou, C.X., Ding, X.L., Liu, Y.: Fluorescence study on the interaction of bovine serum albumin with *p*-aminoazobenzene. *J. Fluoresc.* **18**, 109–118 (2008)